THE JOURNAL OF NAVIGATION (2018), **71**, 1589–1598. © The Royal Institute of Navigation 2018
doi:10.1017/S0373463318000516

A Markley Variables-based Attitude Estimation Method Using Optical Flow and a Star Vector for Spinning Spacecraft

Xiaolin Ning[1,2], Zonghe Ding[1], Mingzhu Xu[1], Jiancheng Fang[1,2] and Gang Liu[1,2]

[1](*School of Instrumentation Science & Opto-electronics Engineering, BeiHang University (BUAA), Beijing 100191, China*)
[2](*Science and Technology on Inertial Laboratory, Fundamental Science on Novel Inertial Instrument & Navigation System Technology Laboratory, Beijing 100191, China*)
(E-mail: celenavbuaa@sina.cn)

Markley variables have advantages of slow variation, easy numerical integration and high precision in describing the attitude of spinning spacecraft. Previous attitude estimation methods based on Markley variables for spinning spacecraft usually employ a sun vector from the sun sensor, a magnetic vector from the magnetometer, or the angular rate from the gyro as the measurement. This paper proposes a Markley variables-based attitude estimation method using optical flow and a star vector from a star sensor as the measurement, where optical flow provides rate information and the star vector provides direction information. This method can estimate the direction of the spin axis and spin angular rate very well by using only one star sensor. In addition, the star sensor has higher accuracy than the traditional sun sensor and magnetometer, and the star sensor can also replace the gyro in case the gyro is out of action. The impact factors of this method are also analysed, which include spin angular rate, spin axis orientation and spacecraft moment of inertia tensor error.

KEYWORDS

1. Spinning spacecraft. 2. Markley variables. 3. Optical flow. 4. Star vector. 5. Attitude estimation.

Submitted: 22 October 2017. Accepted: 21 June 2018. First published online: 6 August 2018.

1. INTRODUCTION. Spin stabilisation is a common attitude control method for spacecraft (Soken et al., 2016). It is usually used on micro-satellites and nanosatellites for its simple implementation and low-energy cost (Slavinskis et al., 2014). In 1993, Markley proposed variables including seven angular momentum parameters to estimate the attitude of spinning spacecraft (Markley, 1993); these vary slowly and are easy to integrate numerically (Sedlak, 2005). The attitude estimation methods using Markley variables are

https://doi.org/10.1017/S0373463318000516 Published online by Cambridge University Press

given the generic name Spin Kalman Filter (SpinKF). Some different versions of SpinKF can be obtained depending on the choice of the error state. When the angular momentum error vector in the inertial reference frame is chosen, the SpinKF is called SpinKF-I, where I refers to the inertial reference frame. Whereas when the angular momentum error vector in the body reference frame is chosen, the SpinKF is called SpinKF-B, where B refers to the body reference frame. (Markley and Sedlak, 2008). Markley and Sedlak (2008) illustrated that SpinKF-I shows a better robustness and efficiency than some other methods. The attitude estimation methods based on Markley variables for spinning spacecraft often employ a combination of magnetometer, sun sensor and gyro (Sedlak, 2005; Markley and Sedlak, 2007; 2008; Ha, 2010). However, a star sensor can replace the combination of a magnetometer, sun sensor and gyro by using a star vector and optical flow as measurement. Optical flow is defined as a Two-Dimensional (2D) rate vector which arises from either the motion of the objects in the scene or the motion of the sensor (Kumar et al., 2016). The motion can be calculated using optical flow between two image frames or a sequence of frames without any prior knowledge (Chen et al., 2013). Optical flow has been used on the angular rate estimation of three-axis spacecraft (Fasano et al., 2013; Pal and Bhat, 2013). Similarly, optical flow can also provide rate information on the attitude estimation for spinning spacecraft.

This paper presents a Markley variables-based attitude estimation method for spinning spacecraft using optical flow and a star vector from a star sensor. Simulations show that the estimation accuracy of the spin axis and spin angular rate can be improved by using optical flow and a star vector as measurements.

2. SYSTEM MODELS OF THE MARKLEY VARIABLES-BASED ATTITUDE ESTIMATION METHOD USING OPTICAL FLOW AND STAR VECTOR.

2.1. *State model.* The Markley variables include $\boldsymbol{L}_B$, L_I and ζ. $\boldsymbol{L}_B$ and $\boldsymbol{L}_I$ are the angular momentum of the spacecraft in the body frame and inertial frame, respectively. ζ is the rotation angle of the spacecraft. The Markley variables $\boldsymbol{L}_B$, $\boldsymbol{L}_I$ and ζ obey the following equations of motion (Sedlak, 2005; Markley and Sedlak, 2008):

$$\begin{aligned} \dot{\boldsymbol{L}}_B &= \boldsymbol{N}_B - \boldsymbol{\omega}_{BI} \times \boldsymbol{L}_B \\ \dot{\boldsymbol{L}}_I &= \boldsymbol{N}_I = \boldsymbol{R}_{BI}^T \boldsymbol{N}_B \\ \dot{\zeta} &= \frac{L[(\boldsymbol{L}_B + \boldsymbol{L}_I) \cdot \boldsymbol{\omega}_{BI} + L^{-2}(\boldsymbol{L}_B \times \boldsymbol{L}_I) \cdot (\boldsymbol{N}_B + \boldsymbol{N}_I)}{L^2 + \boldsymbol{L}_B \cdot \boldsymbol{L}_I} \end{aligned} \tag{1}$$

where $\boldsymbol{N}_B$ and $\boldsymbol{N}_I$ are the total external torque of the spacecraft in the body frame and in the inertial frame, respectively. $\boldsymbol{\omega}_{BI} = [\omega_1 \ \ \omega_2 \ \ \omega_3]^T$, ω_1, ω_2 and ω_3 are the angular rate of the spacecraft around the x-axis, y-axis and z-axis in the body frame, respectively. $\boldsymbol{\omega}_{BI}$ can be given by:

$$\boldsymbol{\omega}_{BI} = \boldsymbol{J}^{-1}(\boldsymbol{L}_B - \boldsymbol{h}) \tag{2}$$

where $\boldsymbol{J}$ is the spacecraft moment of inertia tensor and $\boldsymbol{h}$ is the angular momentum relative to the spacecraft of any moving components (reaction wheels, antennae or solar arrays, etc).

In Equation (1), $L = \|\boldsymbol{L}_B\| = \|\boldsymbol{L}_I\|$. $\boldsymbol{R}_{BI}$ is the inertial-to-body attitude matrix of the spacecraft (He et al., 2017), which can be obtained by two rotations based on the Markley

https://doi.org/10.1017/S0373463318000516 Published online by Cambridge University Press

variables as follows:

$$\boldsymbol{R}_{BI} = \boldsymbol{R}_2\boldsymbol{R}_1 \tag{3}$$

According to the representation of a rotation matrix based on the Euler axis/angle (Shuster, 1993), we have:

$$\boldsymbol{R}_1 = (\cos\zeta)\boldsymbol{I}_{3\times3} + (1-\cos\zeta)\boldsymbol{L}_{Ie}\boldsymbol{L}_{Ie}^T - (\sin\zeta)[\boldsymbol{L}_{Ie}\times] \tag{4}$$

$$\boldsymbol{R}_2 = (\boldsymbol{L}_{Be}\cdot\boldsymbol{L}_{Ie})\boldsymbol{I}_{3\times3} - \boldsymbol{L}_{Ie}\boldsymbol{L}_{Be}^T + \boldsymbol{L}_{Be}\boldsymbol{L}_{Ie}^T + (1+\boldsymbol{L}_{Be}\cdot\boldsymbol{L}_{Ie})^{-1}(\boldsymbol{L}_{Be}\times\boldsymbol{L}_{Ie})(\boldsymbol{L}_{Be}\times\boldsymbol{L}_{Ie})^T \tag{5}$$

where the unit vectors of angular momentum are $\boldsymbol{L}_{Be} = \boldsymbol{L}_B/L$ and $\boldsymbol{L}_{Ie} = L_1/L$. $[\boldsymbol{L}_{Ie}\times]$ is the cross-product matrix.

The state vector is $\boldsymbol{X} = [\boldsymbol{L}_B^T \;\; \boldsymbol{L}_I^T \;\; \zeta]^T$. According to Equation (1), the state model based on Markley variables with process noise $\boldsymbol{w}(t)$ can be abbreviated as:

$$\dot{\boldsymbol{X}} = f(\boldsymbol{X}, t) + \boldsymbol{w}(t) \tag{6}$$

2.2. *Measurement model of optical flow.* The rotation of a spacecraft carrying a star sensor will make the star on the image move from one point to another. The movement of the star points generates optical flow of the star image. Thus, optical flow is considered as a 2D rate vector of stars in a star image which arises from the motion of a star sensor.

2.2.1. *Measurement acquisition.* Assuming there are m matching stars in two successive star images, the image coordinates of the ith star at time t_k and t_{K-1} are $[x_i(k), y_i(k)]$ and $[x_i(k-1), y_i(k-1)]$ $(i = 1, 2, \ldots, \mathrm{m})$, which can be obtained through star centroid extraction and star matching. The optical flow $(u_i(k), v_i(k))$ of the ith star at time t_k can be acquired from two successive star images at time t_k and t_{k-1} by differentiating the star coordinates as follows:

$$\begin{bmatrix} u_i(k) \\ v_i(k) \end{bmatrix} = \begin{bmatrix} \dot{x}_i(k) \\ \dot{y}_i(k) \end{bmatrix} \approx \frac{1}{\Delta T}\begin{bmatrix} x_i(k) - x_i(k-1) + \varepsilon_{x_i}(k) - \varepsilon_{x_i}(k-1) \\ y_i(k) - y_i(k-1) + \varepsilon_{y_i}(k) - \varepsilon_{y_i}(k-1) \end{bmatrix} \tag{7}$$

where the sampling period of the star sensor is $\Delta T = t_k - t_{k-1}$. ε_{x_i} and ε_{y_i} are the measurement noise in the x and y directions, respectively. Therefore, the measurement vector $\boldsymbol{Z}_1(k)$ using the optical flow of stars is:

$$\boldsymbol{Z}_1(k) = [u_1(k) \;\; v_1(k) \;\; u_2(k) \;\; v_2(k) \;\; \cdots \;\; u_m(k) \;\; v_m(k)]^T. \tag{8}$$

2.2.2. *Measurement model.* The coordinates of a unit star vector $(\boldsymbol{r}_c)$ in a camera frame are $[X_c, Y_c, Z_c]^T$ and its 2D image coordinates in a star image are $[x, y]^T$. In the pinhole camera model, the relationship between x, y and $\boldsymbol{r}_c$ is:

$$\begin{aligned} x &= -f\frac{X_e}{Z_e} \\ y &= -f\frac{Y_e}{Z_e} \end{aligned} \tag{9}$$

where f is the focal length of the star sensor.

https://doi.org/10.1017/S0373463318000516 Published online by Cambridge University Press

The movement equation of the spacecraft (Pal and Bhat, 2013) is:

$$\dot{\boldsymbol{r}}_c + \boldsymbol{\omega}_{BI} \times \boldsymbol{r}_c = \dot{\boldsymbol{r}}_i = 0 \tag{10}$$

where r_i is the star vector in the inertial frame corresponding to $\boldsymbol{r}_c$. The component form of Equation (10) is:

$$\begin{cases} \dot{X}_c = \omega_3 Y_c - \omega_2 Z_c \\ \dot{Y}_c = -\omega_3 X_c + \omega_1 Z_c \\ \dot{Z}_c = \omega_2 X_c - \omega_1 Y_c \end{cases} \tag{11}$$

According to Equations (9) and (11), the optical flow vector is:

$$\begin{cases} u = \dot{x} = f\left[-\dfrac{xy}{f^2}\omega_1 + \left(1 + \dfrac{x^2}{f^2}\right)\omega_2 + \dfrac{y}{f}\omega_3\right] \\ v = \dot{y} = f\left[-\left(1 + \dfrac{y^2}{f^2}\right)\omega_1 + \dfrac{xy}{f^2}\omega_2 - \dfrac{x}{f}\omega_3\right] \end{cases} \tag{12}$$

For all the m matching stars in the star image, we have:

$$[u_1 \;\; v_1 \;\; u_2 \;\; v_2 \;\; \cdots \; u_m \;\; v_m]^T = \boldsymbol{H}_1 \boldsymbol{\omega}_{BI} \tag{13}$$

where:

$$\boldsymbol{H}_1 = \left[\boldsymbol{H}^1 \;\; \boldsymbol{H}^2 \;\; \cdots \;\; \boldsymbol{H}^i \;\; \cdots \;\; \boldsymbol{H}^m\right]^T \tag{14}$$

$$\boldsymbol{H}^i = \begin{bmatrix} -\dfrac{x_i y_i}{f} & f + \dfrac{x_i^2}{f} & y_i \\ -f - \dfrac{y_i^2}{f} & \dfrac{x_i y_i}{f} & -x_i \end{bmatrix} \tag{15}$$

According to Equations (2) and (13), the relationship between optical flow and the Markley variables can be given by:

$$[u_1 \;\; v_1 \;\; u_2 \;\; v_2 \;\; \cdots \; u_m \;\; u_m]^T = \boldsymbol{H}_1 \boldsymbol{J}^{-1}(\boldsymbol{L}_B - \boldsymbol{h}) = \boldsymbol{H}_{1x}\boldsymbol{X} - \boldsymbol{H}_0 \boldsymbol{h} \tag{16}$$

where:

$$\boldsymbol{H}_{1x} = [\boldsymbol{H}_0 \;\; 0_{2m\times 3} \;\; 0_{2m\times 1}], \boldsymbol{H}_0 = \boldsymbol{H}_1 \boldsymbol{J}^{-1} \tag{17}$$

According to Equation (16), the measurement model of optical flow is

$$\boldsymbol{Z}_1 = h_1(\boldsymbol{X}) + \boldsymbol{V}_1 \tag{18}$$

where $\boldsymbol{V}_1$ is the measurement noise of optical flow, which is assumed to be zero-mean white Gaussian noise, whose variance matrix is $\boldsymbol{R}_1 = \frac{2}{\Delta T^2} diag\left\{\varepsilon_{x_1}^2, \varepsilon_{y_1}^2, \varepsilon_{x_2}^2, \varepsilon_{y_2}^2, \cdots, \varepsilon_{x_m}^2, \varepsilon_{y_m}^2\right\}$ (Pal and Bhat, 2013).

2.3. *Measurement model of star vector.*

2.3.1. *Measurement acquisition.* In this model, the matching star vector $\boldsymbol{r}_c(k)$ in the camera frame at time t_k is directly considered as the measurement. Thus, the measurement vector $Z_2(k)$ using the star vector is:

$$\boldsymbol{Z}_2(k) = \left[\boldsymbol{r}_c^1(k) \;\; r_c^2(k) \;\; \cdots \;\; r_c^m(k)\right]^T \tag{19}$$

https://doi.org/10.1017/S0373463318000516 Published online by Cambridge University Press

2.3.2. *Measurement model.* The star vector $\boldsymbol{r}_c$ in the camera frame can be derived from the image coordinates of the star. The star vector $\boldsymbol{r}_i$ corresponding to $\boldsymbol{r}_c$ in the inertial frame can be obtained through star identification. The relationship between $\boldsymbol{r}_c$ and $\boldsymbol{r}_i$ is:

$$\boldsymbol{r}_c = \boldsymbol{R}_{BI}\boldsymbol{r}_i \tag{20}$$

From Equations (3) and (20), the measurement model using the star vector can be abbreviated as:

$$\boldsymbol{Z}_2 = h_2(\boldsymbol{X}) + \boldsymbol{V}_2 \tag{21}$$

where $\boldsymbol{V}_2$ is the measurement noise of the star vector, whose variance matrix is $\boldsymbol{R}_2$.

3. THE REDUCED DIMENSION EKF USING OPTICAL FLOW AND A STAR VECTOR. Since the measurement equation in this paper is nonlinear, an Extended Kalman Filter (EKF) is adopted as a navigation filter (Simon, 2006). From the state equation (Equation (6)) and the measurement equation (Equations (18) or (21)), we can formulate the optimal filter.

Markley variables have seven dimensions, and the state error vector is $\Delta\boldsymbol{X} = \boldsymbol{X} - \hat{\boldsymbol{X}}$, where $\hat{\boldsymbol{X}}$ is the current estimation of $\boldsymbol{X}$. Note that an overbar will always denote the current estimate in the subsequent sections. However, there are only five independent variables in six elements of $\boldsymbol{L}_B$ and $\boldsymbol{L}_I$ due to the constraint ($\|\boldsymbol{L}_B\| = \|\boldsymbol{L}_I\| = L$). Therefore, we employ the SpinKF-I method of Markley and Sedlak (2008) to reduce the dimensions of the state error vector in this paper. The six-dimensional error vector $\Delta\boldsymbol{Y} = [\Delta\boldsymbol{\theta}^T \quad \Delta\boldsymbol{L}_I{}^T]^T$ is considered as the new state error vector, where $\Delta\boldsymbol{\theta}$ is the attitude error angle in the body frame and $\Delta\boldsymbol{L}_I$ is the angular momentum error of the spacecraft in the inertial frame. The relationship between $\Delta\boldsymbol{X}$ and $\Delta\boldsymbol{Y}$ is:

$$\Delta\boldsymbol{X} = \boldsymbol{S}\Delta\boldsymbol{Y} \tag{22}$$

$$\boldsymbol{S} = \begin{bmatrix} [\hat{\boldsymbol{L}}_B\times] & \boldsymbol{R}_{BI}(\hat{\boldsymbol{X}}) \\ \boldsymbol{0}_{3\times3} & \boldsymbol{I}_{3\times3} \\ (\hat{\boldsymbol{L}}_{Be} - \hat{\boldsymbol{L}}_{Be}\times\hat{\boldsymbol{w}})^T & \hat{L}^{-1}[\hat{\boldsymbol{w}} + \boldsymbol{R}_{BI}^T(\hat{\boldsymbol{X}})\hat{\boldsymbol{w}}]^T \end{bmatrix} \tag{23}$$

where $\hat{\boldsymbol{w}} = (1 + \hat{\boldsymbol{L}}_{Be}\cdot\hat{\boldsymbol{L}}_{Ie})^{-1}(\hat{\boldsymbol{L}}_{Be}\times\hat{\boldsymbol{L}}_{Ie})$, $\boldsymbol{R}_{BI}(\hat{\boldsymbol{X}}) = \boldsymbol{R}_{BI}\Big\|_{\boldsymbol{X}=\hat{\boldsymbol{X}}}$.

3.1. *The reduced dimension measurement matrix.*

3.1.1. *The reduced dimension measurement matrix of optical flow ($\boldsymbol{H}_{1y}$).* We define the measurement matrix using the optical flow of stars after the number of dimensions is reduced as $\boldsymbol{H}_{1y}$. According to Equations (17) and (23), H_{1y} can be derived as follows:

$$\boldsymbol{H}_{1y} = \boldsymbol{H}_{1x}\boldsymbol{S} = \boldsymbol{H}_1\boldsymbol{J}^{-1}\left[\left[\hat{\boldsymbol{L}}_B\times\right]\boldsymbol{R}_{BI}(\hat{\boldsymbol{X}})\right]. \tag{24}$$

3.1.2. *The reduced dimension measurement matrix of the star vector ($\boldsymbol{H}_{2y}$).* We define the measurement matrix using the star vector after the dimensions are reduced as $\boldsymbol{H}_{2y}$, which is:

$$\boldsymbol{H}_{2y} = \begin{bmatrix} H_{2y}^1 & H_{2y}^2 & \cdots & H_{2y}^i & \cdots & \boldsymbol{H}_{2y}^m \end{bmatrix}^T \tag{25}$$

where $\boldsymbol{H}_{2y}^i$ can be derived from Markley and Sedlak (2008) as follows:

$$\boldsymbol{H}_{2y}^i = [[(R_{BI}(\hat{\boldsymbol{X}})\boldsymbol{r}_i^i)\times] \quad \boldsymbol{0}_{3\times3}] \tag{26}$$

https://doi.org/10.1017/S0373463318000516 Published online by Cambridge University Press

4. SIMULATIONS AND ANALYSIS. In order to demonstrate the feasibility and effectiveness of the proposed method, the performance of three methods are compared by simulations, including a method using only Optical Flow as the measurement (OF method), a method using only a Star Vector as the measurement (SV method) and the proposed method using both Optical Flow and a Star Vector as the measurement (OFSV method). Moreover, we will analyse some impact factors of the proposed method, including spin angular rate, spin axis orientation and spacecraft moment of inertia tensor error.

4.1. *Simulation conditions.* The simulation parameters are based on the Chinese FY-2 meteorological satellite. The right ascension and declination of the rotation axis of FY-2 are 83·7315° and −89·2180° (Li et al., 2005), respectively. The corresponding direction vector of the rotation axis is $e = [0{\cdot}0015, 0{\cdot}0136, -0{\cdot}9999]^T$. The spin angular rate is 0·06°/s. The inertia tensor is $\boldsymbol{J} = diag[13\ 13\ 22] kg \cdot m^2$. The initial attitude angles of pitch, roll and yaw are 0°, 179·218° and 83·7315°, respectively (Ning et al., 2013).

The optical axis of the star sensor is parallel to the rotation axis of FY-2. The star sensor employs a 10° × 10° Field Of View (FOV) with a 1024 pixel × 1024 pixel image plane. It has a 10 Hz sampling frequency, and the visual magnitude (Mv) is 6·0. The element size is 14·7 μm × 14·7 μm. The star location errors are regarded as Gaussian noise with a mean of 0 pixels and a standard deviation of 0·05 pixels.

The filtering period of the reduced dimension EKF is 0·1 s.

The initial state vector is:

$$\boldsymbol{X}_0 = \big[0\, kg \cdot m^2/s, 0\, kg \cdot m^2/s, 0{\cdot}23\, kg \cdot m^2/s, 0\, kg \cdot m^2/s, 0\, kg \cdot m^2/s, -0{\cdot}23\, kg \cdot m^2/s, 0\,\text{rad}\big].$$

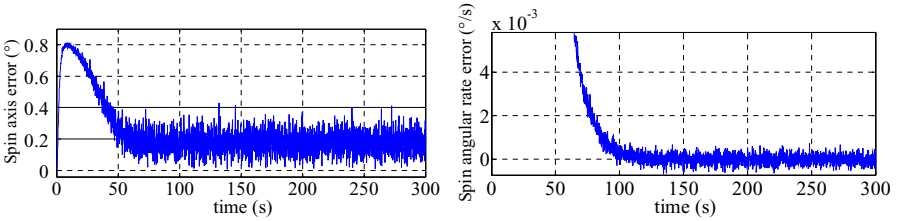
4.2. *Results and analysis.*

4.2.1. *Performance comparison of the three methods.* The estimation error of the spin axis (the angle between the estimated spin axis and the real spin axis) and the estimation error of the spin angular rate using three different methods are shown in Figure 1 and Table 1. It can be seen that the estimation of the spin axis using the OF method is worse than using the SV method, while the estimation of the spin angular rate using the OF method is better than using the SV method. The reason is that the directional vector information from the star vector facilitates the determination of the spin axis, while the rate information from optical flow facilitates the estimation of the spin angular rate. The estimation accuracy of the OFSV method using both the spin axis and spin angular rate is the best among the three methods. The convergence rates of the SV method and the OFSV method are better than the OF method. The results demonstrate that the proposed method using optical flow and a star vector as measurement is an attractive choice for attitude estimation of a spinning spacecraft.

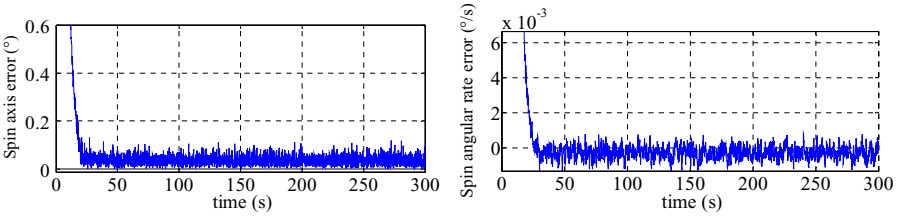
4.2.2. *The impact factors of the proposed method using optical flow and a star vector.* Some factors which affect the performance of the proposed method are analysed in this section, including spin angular rate, spin axis orientation and spacecraft moment of inertia tensor error.

4.2.2.1. *The impact of the spin angular rate.* Currently, the dynamic performance of the star sensor can reach 2°/s. Therefore, the spin angular rate discussed here is lower than 2°/s and avoids blurring the star image. The estimation error of the spin axis and the spin angular rate under different spin angular rates is shown in Table 2. From Table 2, it can be seen that the estimation error of the spin axis decreases with the increase of the spin

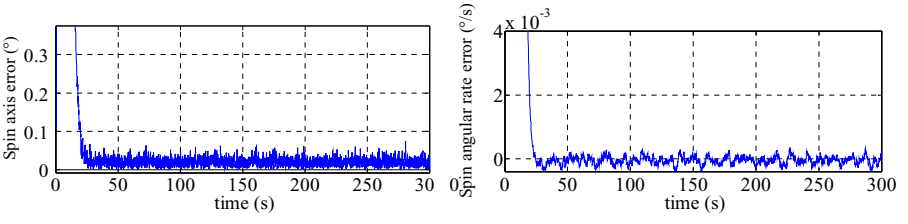
https://doi.org/10.1017/S0373463318000516 Published online by Cambridge University Press



(a) The estimation error of spin axis and spin angular rate of the OF method.



(b) The estimation error of spin axis and spin angular rate of the SV method.



(c) The estimation error of spin axis and spin angular rate of the OFSV method.

Figure 1. The estimation results of three methods.

Table 1. The estimation error of the spin axis and spin angular rate of different methods.

	The estimation error of the spin axis		The estimation error of the spin angular rate	
Method	Mean(°)	RMS(°)	Mean(°/s)	RMS(°/s)
OF	0·177	0·189	$1{\cdot}72 \times 10^{-4}$	$2{\cdot}16 \times 10^{-4}$
SV	0·037	0·042	$3{\cdot}76 \times 10^{-4}$	$4{\cdot}56 \times 10^{-4}$
OFSV	0·020	0·023	$1{\cdot}05 \times 10^{-4}$	$1{\cdot}32 \times 10^{-4}$

angular rate, while the estimation error of the spin angular rate hardly changes. The reason is that the variation of star coordinates in the sequential star images is at the same level of measurement noise under a small angular rate, which reduces the estimation accuracy of the spin axis.

4.2.2.2. *The impact of spin axis orientation.* The spin axis orientation of a spacecraft varies due to requirements of different tasks, which leads to different angles between $\boldsymbol{L}_B$ and $\boldsymbol{L}_I$. The estimation error of the spin axis and spin angular rate under different spin axis orientations is shown in Table 3. Table 3 also shows the number of stars in the FOV under different spin axis orientation. From Table 3, we can see that the estimation accuracy of the spin axis and the spin angular rate barely varies, as the angle between $\boldsymbol{L}_B$ and $\boldsymbol{L}_I$ varies from 0° to 90°. The reason for the slight difference in accuracy is that the number of stars in the

https://doi.org/10.1017/S0373463318000516 Published online by Cambridge University Press

Table 2. Estimation error of spin axis and spin angular rate under different spin angular rates.

spin angular rate(°/s)	The estimation error of the spin axis		The estimation error of the spin angular rate	
	Mean(°)	RMS(°)	Mean(°/s)	RMS(°/s)
0·05	0·025	0·028	$1{\cdot}14 \times 10^{-4}$	$1{\cdot}42 \times 10^{-4}$
0·10	0·012	0·014	$9{\cdot}78 \times 10^{-5}$	$1{\cdot}22 \times 10^{-4}$
0·50	$2{\cdot}41 \times 10^{-3}$	$2{\cdot}73 \times 10^{-3}$	$9{\cdot}67 \times 10^{-5}$	$1{\cdot}17 \times 10^{-4}$
1·00	$1{\cdot}21 \times 10^{-3}$	$1{\cdot}37 \times 10^{-3}$	$9{\cdot}33 \times 10^{-5}$	$1{\cdot}17 \times 10^{-4}$
2·00	$6{\cdot}23 \times 10^{-4}$	$7{\cdot}04 \times 10^{-4}$	$9{\cdot}36 \times 10^{-5}$	$1{\cdot}18 \times 10^{-4}$

Table 3. The estimation error of the spin axis and spin angular rate under different spin axis orientations.

Spin axis orientation	Angle between L_B and L_I/(°)	The number of stars in FOV	Estimation error of the spin axis		Estimation error of the the spin angular rate	
			Mean(°)	RMS(°)	Mean(°/s)	RMS(°/s)
$[0\ \ 0\ \ 1]^T$	0	9	0·020	0·022	$9{\cdot}50 \times 10^{-5}$	$1{\cdot}18 \times 10^{-4}$
$[0\ \ 0{\cdot}4226\ \ 0{\cdot}9063]^T$	25	6	0·021	0·024	$1{\cdot}07 \times 10^{-4}$	$1{\cdot}32 \times 10^{-4}$
$[0\ \ 0{\cdot}7071\ \ 0{\cdot}7071]^T$	45	6	0·021	0·024	$1{\cdot}11 \times 10^{-4}$	$1{\cdot}38 \times 10^{-4}$
$[0\ \ 0{\cdot}9659\ \ 0{\cdot}2588]^T$	75	21	0·018	0·020	$7{\cdot}58 \times 10^{-5}$	$9{\cdot}53 \times 10^{-5}$
$[0\ \ 1\ \ 6{\cdot}1232 \times 10^{-17}]^T$	90	16	0·018	0·021	$8{\cdot}78 \times 10^{-5}$	$1{\cdot}10 \times 10^{-4}$

Table 4. The estimation error of the spin axis and spin angular rate under different inertia tensors.

Inertia tensor ($kg \cdot m^2$)	The estimation error of the spin axis		The estimation error of the spin angular rate	
	Mean(°)	RMS(°)	Mean(°/s)	RMS(°/s)
$\begin{bmatrix} 13 & 0 & 0 \\ 0 & 13 & 0 \\ 0 & 0 & 22 \end{bmatrix}$	0·020	0·023	$1{\cdot}05 \times 10^{-4}$	$1{\cdot}32 \times 10^{-4}$
$\begin{bmatrix} 13 & -0{\cdot}03 & -0{\cdot}02 \\ -0{\cdot}03 & 13 & -0{\cdot}01 \\ -0{\cdot}02 & -0{\cdot}01 & 22 \end{bmatrix}$	0·060	0·062	$1{\cdot}05 \times 10^{-4}$	$1{\cdot}32 \times 10^{-4}$
$\begin{bmatrix} 13 & -0{\cdot}3 & -0{\cdot}2 \\ -0{\cdot}3 & 13 & -0{\cdot}1 \\ -0{\cdot}2 & -0{\cdot}1 & 22 \end{bmatrix}$	0·58	0·58	$1{\cdot}05 \times 10^{-4}$	$1{\cdot}32 \times 10^{-4}$
$\begin{bmatrix} 13 & -3 & -2 \\ -3 & 13 & -1 \\ -2 & -1 & 22 \end{bmatrix}$	5·80	5·80	$9{\cdot}85 \times 10^{-5}$	$1{\cdot}24 \times 10^{-4}$

FOV is different. The more stars in the FOV, the better the estimation accuracy. Therefore, the proposed method has a robust performance in terms of spin axis orientation.

4.2.2.3. *The impact of spacecraft moment of inertia tensor error.* The estimation error of the spin axis and the spin angular rate under different inertia tensors is shown in Table 4. From Table 4, it can be seen that the estimation error of the spin axis increases greatly with the increase in error of the spacecraft moment of inertia tensor, while the estimation error of spin angular rate changes only slightly. This indicates that the proposed method has a

https://doi.org/10.1017/S0373463318000516 Published online by Cambridge University Press

robust performance in the estimation of the spin angular rate in terms of inertia tensor error, while the performance in spin axis estimation is seriously affected by inertia tensor error.

5. CONCLUSIONS. In this paper, a Markley variables-based attitude estimation method using optical flow and a star vector from a star sensor for spinning spacecraft is proposed. Only one star sensor is needed because we can get directional vector information from the star vector and rate information from optical flow, which is equivalent to a combination of a sun sensor, magnetometer and gyro. In addition, the star sensor has a higher accuracy of attitude estimation than the traditional sun sensor and magnetometer, and the star sensor can also replace the gyro in case it is out of action. Simulations reveal that the estimation of the spin axis by the method using only optical flow as the measurement is worse than that of the method only using a star vector as the measurement, while the estimation of the spin angular rate by the method using only optical flow is better than that of the method only using the star vector. The estimation accuracy of both the spin axis and the spin angular rate can be improved by the proposed method using both optical flow and a star vector as the measurements.

ACKNOWLEDGEMENTS

The research presented in this paper has been supported by the National Natural Science Foundation of China (61503013, 61722301) and the grant of the National Basic Research Program of China (973 Program 2014CB744202). The authors wish to express their gratitude to all members of the Science & Technology on Inertial Laboratory, Fundamental Science on Novel Inertial Instrument & Navigation System Technology Laboratory.

REFERENCES

Chen, F., Kang, D. J. and Park, J. H. (2013). New measurement method of Poisson's ratio of PVA hydrogels using an optical flow analysis for a digital imaging system. *Measurement Science & Technology*, **24**(5), 215–220.

Fasano, G., Rufino, G., Accardo, D. and Grassi, M. (2013). Satellite angular velocity estimation based on star images and optical flow techniques. *Sensors*, **13**(10), 12771–12793.

Ha, J. C. V. D (2010). Spin-Axis Attitude Determination Using In-Flight Data. *Journal of Guidance Control & Dynamics*, **33**(3), 768–781.

He, W., Yan, Z., Sun, C. and Chen, Y. (2017). Adaptive Neural Network Control of a Flapping Wing Micro Aerial Vehicle With Disturbance Observer. *IEEE Transactions on Cybernetics*, **47**(10), 3452–3465.

Kumar, P., Kumar, S. and Raman, B. (2016). A fractional order variational model for the robust estimation of optical flow from image sequences. *Optik-International Journal for Light and Electron Optics*, **127**(20), 8710–8727.

Li, Y., Yi, K. and Guan, P. (2005). The determination of attitude and control strategies for double spin geostationary satellites. *Journal of Spacecraft TT& C Technology*, **24**(5), 19–26.

Markley, F. L. (1993). New dynamic variables for momentum-bias spacecraft. *Journal of the Astronautical Sciences*, **41**(4), 557–567.

Markley, F. L. and Sedlak, J. E. (2007). Kalman Filter for Spinning Spacecraft Attitude Estimation. *AIAA Guidance, Navigation, and Control Conference*, 4608–4623, Hilton Head, SC, United States.

Markley, F. L. and Sedlak, J. E. (2008). Kalman Filter for Spinning Spacecraft Attitude Estimation. *Journal of Guidance Control & Dynamics*, **31**(6), 1750–1760.

Ning, X., Bai, X. and Jiang, L. (2013). New Method for Attitude Determination of Spin Satellite Based on Continuous Star Map Observation. *Chinese Space Science & Technology*, **33**(6), 49–57.

Pal, M. and Bhat, M. S. (2013). Star sensor based spacecraft angular rate estimation independent of attitude determination. *IEEE International Conference on. Control Applications (CCA)*, 580–585, Hyderabad, India.

https://doi.org/10.1017/S0373463318000516 Published online by Cambridge University Press

Sedlak, J. E. (2005). *Spinning Spacecraft Attitude Estimation Using Markley Variables: Filter Implementation and Results*. Nasa Goddard Space Flight Center Cp.

Shuster, M. D. (1993). A survey of attitude representations. *The Journal of the Astronautical Sciences*, **41**(4), 439–517.

Simon, D. (2006). *Optimal State Estimation: Kalman, H Infinity, and Nonlinear Approaches*. Wiley-Interscience.

Slavinskis, A., Kvell, U., Kulu, E., Sünter, I., Kuuste, H., Lätt, S., Voormansik, K. and Noorma, M. (2014). High spin rate magnetic controller for nanosatellites. *Acta Astronautica*, **95**(5), 218–226.

Soken, H. E., Sakai, S., Asamura, K., Nakamura, Y. and Takashima, T. (2016). Spin-Axis Tilt Estimation for Spinning Spacecraft. *AIAA Guidance, Navigation and Control Conference*, 1–15, San Diego, California, USA, doi:10.2514/6.2016-0626.

https://doi.org/10.1017/S0373463318000516 Published online by Cambridge University Press